# Constructing Narrowband Heavy Metal Platinum (II) Complex by Integrating Multiple Resonance Molecular System

*Yu Feng,[a] Xuming Zhuang,[b] Yincai Xu,*[,a] Jianan Xue,[a] Qingyang Wang,[a] Yu Liu*[,a] and Yue Wang*[,a,c]*

[a]Y. Feng, Dr. Y. Xu, J. Xue, Q. Wang, Prof. Y. Liu and Prof. Y. Wang
State Key Laboratory of Supramolecular Structure and Materials
College of Chemistry, Jilin University, Changchun 130012, P. R. China
[b]Dr. X. Zhuang
Jihua Laboratory, 28 Huandao South Road, Foshan 528200, Guangdong Province, P. R. China.
[c]Prof. Y. Wang
Jihua Hengye Electronic Materials CO. LTD., Foshan, 528200, Guangdong Province, P. R. China.
E-mails: ycxu17@mails.jlu.edu.cn, yuliu@jlu.edu.cn, yuewang@jlu.edu.cn

**Keywords**: multiple resonance, phosphorescent metal complexes, narrowband emission

**Abstract**: The narrowband emission required by wide color gamut display is an extremely important research topic for any luminescence mechanism, which has made significant progress in traditional fluorescence and thermally activated delayed fluorescence (TADF) based on purely organic compounds, but is far from mature in phosphorescence based on metal organic complexes. Herein, we propose a feasible molecular design paradigm for constructing the desirable narrowband-emission organic electroluminescence (EL) emitter by integrating an original multi-resonance thermally activated delayed fluorescent (MR-TADF) fragment into the classical heavy metal platinum (II) complex. The target model platinum (II) complex BNCPPt shows

green emission with a single peak at 497 nm and the quite narrow full-width at half-maximum (FWHM) of 27 nm in toluene.

As one of the current mainstream technologies for the small and medium-sized flat panel displays, organic light emitting diode (OLED) has excellent merits of strong flexibility, fast response time, active emitting and vivid color, etc., and thus is gradually popularized in smart phones, curly televisions, artificial intelligence patches and other commercial products. In order to further improve the image quality and reproduce the most authentic colors of nature on the screen, developing the wide color gamut OLED based on ultra-high definition display (UHD) technology has the sufficient scientific attraction as well as meets the strong industrial requirement.[1] As it should be, designing and adopting the emitting materials with the standard emission peak position and possessing the spectral band as narrow as possible is the straightforward and effective approach for that.

Currently, the narrowband materials based on fluorescence emission mechanism have made vigorous development, especially for thermally activated delayed fluorescence (TADF) materials induced by multiple resonance (MR) effects.[2] In MR-TADF system molecules, the highest occupied molecular orbitals (HOMO) and lowest unoccupied molecular orbitals (LUMO) induced by the opposite electronic properties of donors (such as nitrogen, oxygen and sulfur atoms) and acceptors (such as boron and carbonyl groups) are alternately arranged on the atoms, thus integrating the short-range charge delocalization effect and long-range complementary resonance

interaction, and thus resulting in narrowband blue, green and red emission with very high external quantum efficiencies of 30-40%.[3] However, MR-TADF emitting systems usually suffer from the pronounced device efficiency roll-offs of over 20% at the practical luminance of 1000 cd $m^{-2}$ due to the inherent long residence times of triplet excitons. On the other hand, although phosphorescent metal complexes-based OLEDs possess quite comprehensive high electroluminescence (EL) performance in terms of brightness, efficiency and power consumption, they tend to bear broadband emission due to the complex luminescence processes and intermolecular interactions.[4] These original EL spectra thereupon need additional slimming technique such as color filtering or optical microcavity to meet the requirements of commercial display,[5] and thus the certain loss of luminous efficacy and increase of manufacturing cost/power consumption are inevitable. So far, there have been sporadic reports on the spectral narrowing of phosphorescent complexes through introducing the large sterically hindered/rigid groups into the complexes to restrict the free relaxation of ligand and inhibit the intermolecular interactions,[6] which indeed achieve a certain degree of spectral slimming, but further optimization for spectra is still required to match the high-quality display applications, which will be accompanied by additional multistep reaction sequences as well as requirement for harsh purification.

In addition, solution processing technologies including spin coating and ink printing are more promising due to their simple and low-cost fabrication process for large size panel production based on OLED.[7] However, almost all the present

MR-TADF organic molecules and small-molecule phosphorescent complexes are basically designed according to the requirement of thermal-deposition fabrication, thus they are usually easy crystallized based on spin coating process and their film morphology is not stable enough, indicating their inappropriate for wet-process method. Therefore, it is still an enormous challenge to develop new solution processing organic EL material system that can integrate the desirable narrowband emission spectrum and the amazing emitting performance. In this work, as an induced fragment of resonance effect as well as a solubilizing group, our original MR-TADF molecule BNCz[3a] is integrated into the classical cyclometalated (C^N) ligand 2-phenylpyridine (ppy) for constructing a new B-N-embedded ligand BNCP and the corresponding heavy metal platinum (Pt-II) complex BNCPPt. As we expected, both the C^N ligand BNCP and the target complex BNCPPt are upgraded to two emitters with the amazing MR effect. Thus this work enrich the MR-TADF material system by adopting the new chemical structure framework through ingenious optimizing the classical organometallic complex, and more importantly, which exhibits a simple and practical research strategy to develop the promising wet-process MR-TADF material systems those possessing the desirable narrowband emission.

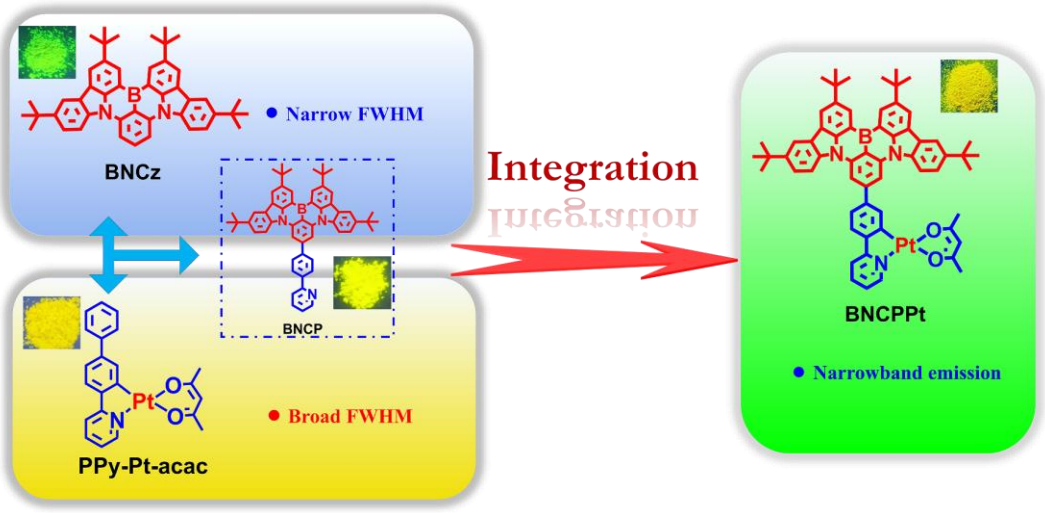


**Scheme 1**. Design concepts and chemical structures of BNCz, PPy-Pt-acac, BNCP and BNCPPt. (Inset: photograph of solid powder taken under 365 nm UV light).

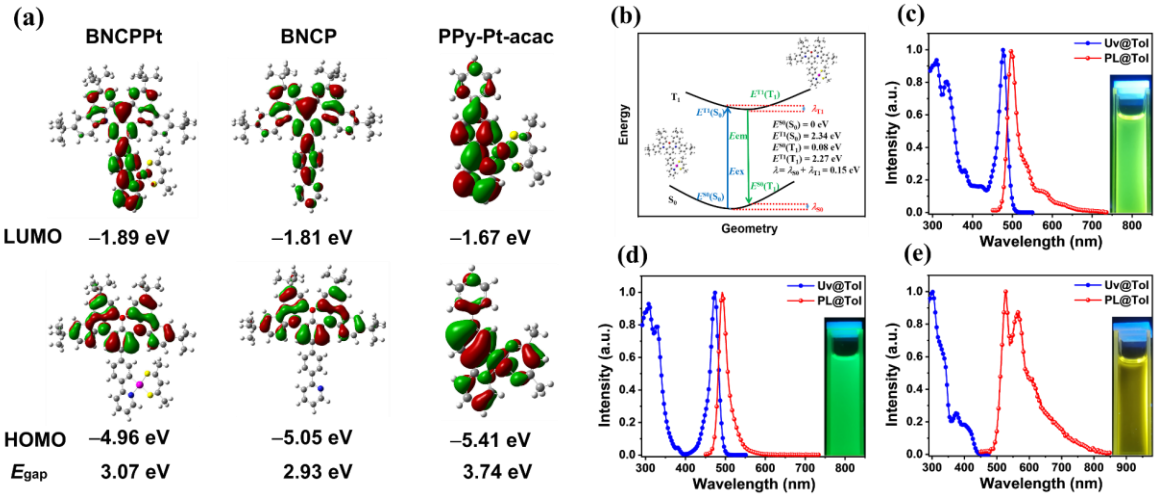


**Figure 1.** a) Calculated electron cloud distribution patterns and energy levels of HOMO and LUMO of BNCPPt, BNCP and PPy-Pt-acac. b) Optimized $S_0$ and $T_1$ structures, single point energies, and reorganization energies ($\lambda$) of BNCPPt. c) Normalized UV–vis absorption and phosphorescence spectra of BNCPPt measured in toluene solution ($1 \times 10^{-5}$ M, 298 K). d) Normalized UV–vis absorption and fluorescence spectra of BNCP measured in toluene solution ($1 \times 10^{-5}$ M, 298 K). e) Normalized UV–vis absorption and phosphorescence spectra of PPy-Pt-acac measured in toluene solution ($1 \times 10^{-5}$ M, 298 K). (Inset: photograph taken under 365 nm UV light).

**Table 1.** Summary of photophysical properties of BNCPPt, BNCP and PPy-Pt-acac.

| compound | $\lambda_{abs}$ [a] [nm] | $\lambda_{em}$ [b] [nm] | FWHM [c] [nm] | HOMO [d] [eV] | LUMO [d] [eV] | $\Phi_{PL}$ [e] [%] |
|---|---|---|---|---|---|---|
| BNCPPt | 310, 334, 380, 422, 478 | 497, 536, 578 | 27 | −4.81 | −2.64 | 75 |
| BNCP | 308, 329, 381, 474 | 493 | 23 | −5.19 | −2.60 | 97 |
| PPy-Pt-acac | 301, 378, 402 | 527, 564, 612 | 78 | −4.74 | −2.36 | 35 |

a) Peak wavelength of absorption peak in toluene solution ($1 \times 10^{-5}$ M, 298 K). b) Peak wavelength of PL spectrum in toluene ($1 \times 10^{-5}$ M, 298 K). c) Full-width at half-maximum. d) Determined from cyclic voltammetry using the formula: $E_{HOMO} = -(E_{ox} + 4.8)$ eV and $E_{LUMO} = -(E_{red} + 4.8)$ eV. e) Absolute photoluminescence quantum yield measured with an integrating sphere system in $N_2$-bubbling toluene.

The C^N ligand BNCP is synthesized from the substrate BNCz *via* an easy two-step handling procedure, including Miyaura boron esterification and Suzuki coupling as shown in **Scheme 1**.[8] The final complex BNCPPt is obtained with the yield of more than 30% by simple reaction of ligand with $K_2PtCl_4$ and auxiliary ligand acetylacetone (acac). The detailed synthesis procedures including NMR, mass spectrometry and elemental analysis are provided in Electronic Supplementary Information (**ESI**) file. For comparison, the reference parent molecule PPy-Pt-acac's chemical structure, synthesis and the corresponding characterization results are also shown here and in **ESI** file. According to the cyclic voltammetry (CV) measurement (**Figure S9** in **ESI**), the HOMO and LUMO energy levels are determined as −4.81 and −2.64 eV for BNCPPt, −5.19 and −2.60 eV for BNCP, −4.74 and −2.36 eV for PPy-Pt-acac. Furthermore, to examine the influence of BNCz group on the optimized molecular structure and frontier molecular orbital distribution, the electron cloud

distributions of three molecules are calculated by density functional theory (DFT) and time-dependent DFT (TD-DFT) at the B3LYP/6-31G(d,p) level. In particular, the heavy platinum atom was calculated by combining the basis set Stuttgart Dresden ECP (SDD). **Figure 1a** shows the electron cloud distributions of HOMO and LUMO and corresponding energy levels and HOMO−LUMO energy level gaps ($E_{gap}$s) for BNCPPt, BNCP and PPy-Pt-acac. The electrostatic potential (ESP) distribution and spin−orbit coupling matrix elements (<S|$\hat{H}_{SOC}$|T>s) are shown in **Figure S10−S11**. The HOMO distributions of BNCPPt and BNCP are similar, which are mainly located on the MR skeleton belong to the C^N ligand. Due to the central platinum ion (II) being introduced, the LUMO of BNCPPt is not only predominately distributed on the ligand BNCP, but also partly extends to the metal ion. According to the theory of constructing charge transfer excited states based on frontier molecular orbital engineering (FMOE),[9] the LUMO in ligand BNCP primarily resides on the MR skeleton, that is, distributed on the boron atom and the carbon atoms at the *ortho*/*para* positions in BNCz moiety, and also extends to the 2-phenylpyridine unit connected to the *para*-carbon position of the B-substituted phenyl ring. Very little contribution of the auxiliary ligand acetylacetone (acac) to the frontier molecular orbital of BNCPPt indicates this molecular segment's influence on the frontier molecular property of the complex should be quite limited.

The C^N ligand BNCP in the complex BNCPPt has the canonical MR effect, which mirrors the short-range charge transfer state.[10] It can be reasonably conjectured that when the MR skeleton is grafted into the heavy atom containing complex, this endows

the complex with a relatively static “breath” movement, which restricts the vigorous molecular stretching vibration of bond and the free relaxation of the complex.[11] The S0 → S1 transition of BNCPPt is attributed to the transition from HOMO to LUMO (see **Table S1−S3**), where the frontier molecular orbitals are principally arranged alternately at boron/nitrogen and carbon atoms of BNCP. Compared with the conventional phosphorescent metal complexes, the metal-to-ligand charge transfer (MLCT) state of BNCPPt is greatly reduced, and the intra-ligand charge transfer transition (ILCT) state plays the most important role. From the result of ESP analysis, the more dispersed electron cloud density in BNCPPt than that in BNCP, pulling down the former LUMO energy level, which moderately enhances the intramolecular charge transfer (ICT) intensity, reduces $E_{gap}$s and generates red-shift emission.

As we know, the molecular reorganization energy (λ) based on the Marcus theory is an important parameter to investigate the geometrical deformation and the emission spectral pattern. In principle, the relatively low recombination energy level is a prerequisite for narrowband emission. The reorganization energies are calculated to be 0.15, 0.14 and 0.59 eV for BNCPPt, BNCP and PPy-Pt-acac, respectively (**Figure 1b** and **Figure S12**). The quite similar value of BNCPPt (0.15 eV) and BNCz (0.13 eV)[8] indicates that this newly-constructed complex may have the desirable narrowband emission curve similar to the latter. According to the decomposition results of the reorganization energy from $T_1$ to $S_0$, the narrow FWHM can be achieved by enhancing low-frequency and suppressing high-frequency vibronic coupling. Here, the observed reorganization energies for the different normal vibration modes of

BNCPPt are mainly located in the low-frequency region (< 500 $cm^{-1}$), which have very small values (< 43 $cm^{-1}$) (see **Figure S13–S14**).[12] Therefore, as mentioned above, the introduction of B-N-embedded MR skeleton into the platinum (II) complex indeed limits the structural deformation between its ground and excited state, thus inhibiting the free relaxation and leading to narrowband emission of the target complex.

The fundamental photophysical properties including ultraviolet–visible (UV–vis) absorption and photoluminescence (PL) spectra of BNCPPt, BNCP and PPy-Pt-acac are measured in dilute toluene at room temperature (**Figure 1c–e** and **Table 1**). The UV–vis absorption curves of BNCPPt and BNCP are similar, where the intense high-energy absorption band between 300 and 370 nm is assigned to the intraligand $\pi \rightarrow \pi^*$ transitions of the conjugated backbone, the moderate absorption bands covering 370–400 and 400–435 nm should be attributed to the MLCT transition, and the strong low-energy band with 435–520 nm for BNCPPt can be ascribed to the ILCT transition as well as the MLCT transition partly. As we expected, BNCPPt exhibits a remarkably light green emission possessing a sharp peak at 497 nm with a quite narrow FWHM of 27 nm, which are similar with those of BNCP (493 nm and 23 nm respectively). They are obviously different from the corresponding parameters of the reference complex PPy-Pt-acac, which shows a double sharp peak at 527 and 564 nm with broader FWHM of 78 nm. Subsequently, in their emission spectra at 77 K (see **Figure S15** and **Table S4**), BNCP and PPy-Pt-acac exhibit almost same curves as the cases at room temperature in **Figure 1**, but BNCPPt show the double peaks with different

emission intensity, where the short-wavelength (～528nm) main peak should be originated from the ILCT transition of the C^N ligand BNCP, and it has the similar emission peak and curve profile to those of BNCP at both at 77 K (**Figure S15b**) and room temperature as shown in **Figure 1c**, and the long-wavelength (～568nm) broad shoulder peak should derive from this complex's MLCT transition, which is consistent with the theoretical calculation results above.

In addition, a series of doped films based on BNCPPt, BNCP and PPy-Pt-acac blended in a mixed host system of mCPBC (9-(3-(9*H*-carbazol-9-yl)phenyl)-9*H*-3,9'-bicarbazole):PIM-TRZ (di-[4-(*N*,*N*-ditolyamino)-phenyl]cyclohexane) (2:1)[13] with a low doping concentrations of 2 wt% are prepared by spin-coating method from fresh cholorobenzene solvent (15 mg/ml) onto quartz substrates, and their PL spectra, transient PL decay profiles, lifetimes, and photoluminescence quantum yields ($\Phi_{PL}$s) are comprehensively studied. All the doped films' PL spectra display slight red-shifts and widened FWHMs (**Figure S16** and **Table S5**) compared with the cases in the dilute solution as shown in **Figure 1**, which should be due to the certain molecular aggregation in these solid films. The transient PL decay curve of BNCPPt doped film shows the clear monoexponential decay with the shortest lifetime value of 3.78 of the and 14.38 μs respectively, and PPy-Pt-acac doped films where there is no other long-lived emissive component such as the phosphorescence can be detected. In comparison, the typical double exponential decay originated from the traditional fluorescence together with the delayed fluorescence emission from BNCP-based

doped film achieves the much longer lifetime of 62.1 μs (see **ESI** file). In summary, these properties of platinum (II) complex BNCPPt have tremendous advantages for the preparation of highly efficient OLED with narrowband emission. The application of these compounds in optoelectronic devices are ongoing in our laboratory.

In conclusion, a representative unique multiple resonance fragment into phosphorescent metal complexes (MR-PMC) comprising of B-N-embedded framework combined with heavy metal platinum atom, has been innovatively constructed. The target model complex BNCPPt is utilized as an emitter that displays green emission with a peak at 497 nm and small FWHM of 27 nm. This kind of complex not only inherits the excellent gene of MR skeleton, but also retains the striking advantages of short lifetime of phosphorescent complexes. Most important of all, this innovative design concept builds a bridge between MR and phosphorescent metal complexes, establishes a concrete molecular structure design paradigm, and provides a novel strategy for the construction of phosphorescent complexes with narrowband emission towards ultra-high definition display.

**Acknowledgements**

Yu Feng and Dr. Xuming Zhuang contributed equally to the work reported in this article. This work was supported by the Jilin Provincial Science and Technology Development Plan Project (20220201085GX) and Programme Chine/Wallonie-Bruxelles de coopération bilatérale de recherche (2021YFE0115700) and National Natural Science Foundation of China-General Program (52173282) and GuangDong Basic and Applied Basic Research Foundation-Key Project of Regional Joint Fund (2020B1515120068).

**Conflict of Interest**

The authors declare no conflict of interest.

**References**

[1] a) C. W. Tang, S. A. VanSlyke, *Appl. Phys. Lett.* **1987**, *51*, 913−915; b) R. M. Soneira, *Inf. Disp.* **2016**, *32*, 26; c) P. Pust, P. J. Schmidt, W. Schnick, *Nat. Mater.* **2015**, *14*, 454−458; d) R. Zhu, Z. Luo, H. Chen, Y. Dong, S.-T. Wu, *Opt. Express.* **2015**, *23*, 23680−23693.

[2] a) H. Uoyama, K. Goushi, K. Shizu, H. Nomura, C. Adachi, *Nature* **2012**, *492*, 234−238; b) Y. Tao, K. Yuan, T. Chen, P. Xu, H. Li, R. Chen, C. Zheng, L. Zhang, W. Huang, *Adv. Mater.* **2014**, *26*, 7931−7958; c) T. Hatakeyama, K. Shiren, K. Nakajima, S. Nomura, S. Nakatsuka, K. Kinoshita, J. Ni, Y. Ono, T. Ikuta, *Adv. Mater.* **2016**, *28*, 2777−2781; d) Z. Yang, Z. Mao, Z. Xie, Y. Zhang, S. Liu, J. Zhao, J. Xu, Z. Chi, M. P. Aldred, *Chem. Soc. Rev.* **2017**, *46*, 915−1016; e) Y. Kondo, K. Yoshiura, S. Kitera, H. Nishi, S. Oda, H. Gotoh, Y. Sasada, M. Yanai, T. Hatakeyama, *Nat. Photonics* **2019**, *13*, 678−682.

[3] a) Y. Xu, Z. Cheng, Z. Li, B. Liang, J. Wang, J. Wei, Z. Zhang, Y. Wang, *Adv. Opt. Mater.* **2020**, *8*, 1902142; b) H. J. Kim, T. Yasuda, *Adv. Opt. Mater.* **2022**, *10*, 2201714; c) S. M. Suresh, E. Duda, D. Hall, Z. Yao, S. Bagnich, A. M. Z. Slawin, H. Bassler, D. Beljonne, M. Buck, Y. Olivier, A. Kohler, E. Zysman-Colman, *J. Am. Chem. Soc.* **2020**, *142*, 6588−6599; d) S. Oda, B. Kawakami, Y. Yamasaki, R. Matsumoto, M. Yoshioka, D. Fukushima, S. Nakatsuka, T. Hatakeyama, *J. Am. Chem. Soc.* **2022**, *144*, 106−112; e) G. Liu, H. Sasabe, K. Kumada, H. Arai, J. Kido, *Chem. Eur. J.* **2022**, *28*, e202201605; f) J. Liu, Y. Zhu, T. Tsuboi, C. Deng, W. Lou, D. Wang, T. Liu, Q. Zhang, *Nat. Commun.* **2022**, *13*, 4876; g) G. Chen, J. Wang, W. C. Chen, Y. Gong, N. Zhuang, H. Liang, L. Xing, Y. Liu, S. Ji, H. L. Zhang, Z. Zhao, Y.

Huo, B. Z. Tang, *Adv. Funct. Mater.* **2023**, 2211893; h) N. Ikeda, S. Oda, R. Matsumoto, M. Yoshioka, D. Fukushima, K. Yoshiura, N. Yasuda, T. Hatakeyama, *Adv. Mater.* **2020**, *32*, 2004072; i) H.-J. Cheon, S.-J. Woo, S.-H. Baek, J.-H. Lee, Y.-H. Kim, *Adv. Mater.* **2022**, *34*, 2207416; j) I. S. Park, M. Yang, H. Shibata, N. Amanokura, T. Yasuda, *Adv. Mater.* **2022**, *34*, 2107951; k) J. Bian, S. Chen, L. Qiu, R. Tian, Y. Man, Y. Wang, S. Chen, J. Zhang, C. Duan, C. Han, H. Xu, *Adv. Mater.* **2022**, *34*, 2110547; l) P. Jiang, J. Miao, X. Cao, H. Xia, K. Pan, T. Hua, X. Lv, Z. Huang, Y. Zou, C. Yang, *Adv. Mater.* **2022**, *34*, 2106954; m) J. Park, K. J. Kim, J. Lim, T. Kim, J. Y. Lee, *Adv. Mater.* **2022**, *34*, 2108581; n) X. Wu, J.-W. Huang, B.-K. Su, S. Wang, L. Yuan, W.-Q. Zheng, H. Zhang, Y.-X. Zheng, W. Zhu, P.-T. Chou, *Adv. Mater.* **2022**, *34*, 2105080; o) Q. Wang, Y. Xu, T. Yang, J. Xue, Y. Wang, *Adv. Mater.* **2023**, *35*, 2205166; p) X. Liang, Z. P. Yan, H. B. Han, Z. G. Wu, Y. X. Zheng, H. Meng, J. L. Zuo, W. Huang, *Angew. Chem. Int. Ed.* **2018**, *57*, 11316–11320; q) Y. Zhang, D. Zhang, J. Wei, X. Hong, Y. Lu, D. Hu, G. Li, Z. Liu, Y. Chen, L. Duan, *Angew. Chem. Int. Ed.* **2020**, *59*, 17499−17503; r) J. A. Knöller, G. Meng, X. Wang, D. Hall, A. Pershin, D. Beljonne, Y. Olivier, S. Laschat, E. Zysman-Colman, S. Wang, *Angew. Chem. Int. Ed.* **2020**, *59*, 3156−3160; s) J.-J. Zhang, L. Yang, F. Liu, Y. Fu, J. Liu, A. A. Popov, J. Ma, X. Feng, *Angew. Chem. Int. Ed.* **2021**, *60*, 25695−25700; t) Y. Liu, X. Xiao, Z. Huang, D. Yang, D. Ma, J. Liu, B. Lei, Z. Bin, J. You, *Angew. Chem. Int. Ed.* **2022**, *61*, e202210210; u) Y.-K. Qu, D.-Y. Zhou, F.-C. Kong, Q. Zheng, X. Tang, Y.-H. Zhu, C.-C. Huang, Z.-Q. Feng, J. Fan, C. Adachi, L.-S. Liao, Z.-Q. Jiang, *Angew. Chem. Int. Ed.* **2022**, *61*, e202201886; v) F. Liu, Z. Cheng, Y.

Jiang, L. Gao, H. Liu, H. Liu, Z. Feng, P. Lu, W. Yang, *Angew. Chem. Int. Ed.* **2022**, *61*, e202116927; w) X. F. Luo, S. Q. Song, H. X. Ni, H. Ma, D. Yang, D. Ma, Y. X. Zheng, J. L. Zuo, *Angew. Chem. Int. Ed.* **2022**, *61*, e202209984; x) S. Cai, G. S. M. Tong, L. Du, G. K.-M. So, F.-F. Hung, T.-L. Lam, G. Cheng, H. Xiao, X. Chang, Z.-X. Xu, C.-M. Che, *Angew. Chem. Int. Ed.* **2022**, *61*, e202213392.

[4] a) Y.-S. Park, S. Lee, K.-H. Kim, S.-Y. Kim, J.-H. Lee, J.-J. Kim, *Adv. Funct. Mater.* **2013**, *23*, 4914-4920; b) T. Fleetham, J. Ecton, Z. Wang, N. Bakken, J. Li, *Adv. Mater.* **2013**, *25*, 2573-2576; c) G. Cheng, S. C. Kui, W.-H. Ang, M.-Y. Ko, P.-K. Chow, C.-L. Kwong, C.-C. Kwok, C. Ma, X. Guan, K.-H. Low, S.-J. Su, C.-M. Che, *Chem. Sci.* **2014**, *5*, 4819−4830; d) S. Shi, M. C. Jung, C. Coburn, A. Tadle, D. Sylvinson MR, P. I. Djurovich, S. R. Forrest, M. E. Thompson, *J. Am. Chem. Soc.* **2019**, *141*, 3576−3588; e) Y. Sun, X. Yang, B. Liu, H. Guo, G. Zhou, W. Ma, Z. Wu, *J. Mate. Chem. C.* **2019**, *7*, 12552−12559; f) G. Li, X. Zhao, T. Fleetham, Q. Chen, F. Zhan, J. Zheng, Y.-F. Yang, W. Lou, Y. Yang, K. Fang, Z. Shao, Q. Zhang, Y. She, *Chem. Mater.* **2019**, *32*, 537−548; g) Y.-C. Wei, S. F. Wang, Y. Hu, L.-S. Liao, D.-G. Chen, K.-H. Chang, C.-W. Wang, S.-H. Liu, W.-H. Chan, J.-L. Liao, W.-Y. Hung, T.-H. Wang, P.-T. Chen, H.-F. Hsu, Y. Chi, P.-T.Chou, *Nat. Photonics* **2020**, *14*, 570−577; h) A. Ying, Y.-H. Huang, C.-H. Lu, Z. Chen, W.-K. Lee, X. Zeng, T. Chen, X. Cao, C.-C. Wu, S. Gong, *ACS Appl. Mater. & Interfaces.* **2021**, *13*, 13478−13486; i) J.-M. Kim, K. Y. Hwang, S. Kim, J. Lim, B. Kang, K. H. Lee, B. Choi, S.-Y. Kwak, J. Y. Lee, *Adv. Sci.* **2022**, *9*, 2203903.

[5] a) N. Takada, T. Tsutsui, S. Saito, *Appl. Phys. Lett.* **1993**, *63*, 2032−2034; b) T.-Y. Cho, C.-L. Lin, C.-C. Wu, *Appl. Phys. Lett.* **2006**, *88*, 111106.

[6] a) X.-J. Liao, J.-J. Zhu, L. Yuan, Z.-P. Yan, Z.-L. Tu, M.-X. Mao, J.-J. Lu, W.-W. Zhang, Y.-X. Zheng, *Mater. Chem. Front.* **2021**, *5*, 6951−6959; b) Z.-Z. Qu, X.-F. Luo, M.-X. Mao, C.-F. Yip, Y.-X. Zheng, J.-L. Zuo, *Adv. Energy Sustainability Res.* **2022**, *3*, 2200057; c) X. Feng, J. G. Yang, J. Miao, C. Zhong, X. Yin, N. Li, C. Wu, Q. Zhang, Y. Chen, K. Li, C. Yang, *Angew. Chem. Int. Ed.* **2022**, *61*, e202209451; d) J. Sun, H. Ahn, S. Kang, S.-B. Ko, D. Song, H. A. Um, S. Kim, Y. Lee, P. Jeon, S.-H. Hwang, Y. You, C. Chu, S. Kim, *Nat. Photonics* **2022**, *16*, 212−218.

[7] a) M. C. Gather, A. Köhnen, K. Meerholz, *Adv. Mater.* **2011**, *23*, 233−248; b) Y. J. Cho, K. S. Yook, J. Y. Lee, *Adv. Mater.* **2014**, *26*, 6642−6646; c) K. S. Yook, J. Y. Lee, *Adv. Mater.* **2014**, *26*, 4218−4233; d) N. Ikeda, S. Oda, R. Matsumoto, M. Yoshioka, D. Fukushima, K. Yoshiura, N. Yasuda, T. Hatakeyama, *Adv. Mater.* **2020**, *32*, 2004072; e) X. Cai, Y. Xu, Y. Pan, L. Li, Y. Pu, X. Zhuang, C. Li, Y. Wang, *Angew. Chem. Int. Ed.* **2023**, *62*, e202216473; f) S. Wang, H. Zhang, B. Zhang, Z. Xie, W.-Y. Wong, *Mater. Sci. Eng. R* **2020**, *140*, 100547; g) J. H. Burroughes, D. D. Bradley, A. Brown, R. Marks, K. Mackay, R. H. Friend, P. L. Burns, A. B. Holmes, *Nature* **1990**, *347*, 539−541; h) C. D. Müller, A. Falcou, N. Reckefuss, M. Rojahn, V. Wiederhirn, P. Rudati, H. Frohne, O. Nuyken, H. Becker, K. Meerholz, *Nature* **2003**, *421*, 829−833.

[8] Y. Xu, C. Li, Z. Li, J. Wang, J. Xue, Q. Wang, X. Cai, Y. Wang, *CCS Chem.* **2022**, *4*, 2065−2079.

[9] a) Y. Zhang, D. Zhang, J. Wei, Z. Liu, Y. Lu, L. Duan, *Angew. Chem. Int. Ed.* **2019**, *58*, 16912−16917; b) Y. Xu, C. Li, Z. Li, Q. Wang, X. Cai, J. Wei, Y. Wang, *Angew. Chem. Int. Ed.* **2020**, *59*, 17442−17446; c) Y. Xu, Q. Wang, X. Cai, C. Li, Y. Wang, A*dv. Mater.* **2021**, *33*, 2100652.

[10] a) S. Wu, W. Li, K. Yoshida, D. Hall, S. M. Suresh, T. Sayner, J. Gong, D. Beljonne, Y. Olivier, I. D. W. Samuel, E. Zysman-Colman, *ACS Appl. Mater. Interfaces* **2022**, *14*, 22341−22352; b) A. Pershin, D. Hall, V. Lemaur, J.-C. Sancho-Garcia, L. Muccioli, E. Zysman-Colman, D. Beljonne, Y. Olivier, *Nat. Commun.* **2019**, *10*, 597.

[11] X. Qiu, G. Tian, C. Lin, Y. Pan, X. Ye, B. Wang, D. Ma, D. Hu, Y. Luo, Y. Ma, *Adv. Opt. Mater.* **2021**, *9*, 2001845.

[12] Bolla, G.; Liao, Q.; Amirjalayer, S.; Tu, Z.; Lv, S.; Liu, J.; Zhang, S.; Zhen, Y.; Yi, Y.; Liu, X.; Fu, H.; Fuchs, H.; Dong, H.; Wang, Z.; Hu, W, *Angew. Chem. Int. Ed.* **2021**, *60*, 281–289.

[13] B. Liang, J. Wang, Z. Cheng, J. Wei, Y. Wang, *J. Phys. Chem. Lett.* **2019**, *10*, 2811–2816.

***Table of contents***

A novel molecular design paradigm for narrowband phosphorescence organic light emitting diodes (OLEDs) based on integrating multiple resonance fragment into phosphorescent metal complexes (MR-PMC) has been proposed, and a representative platinum (II) complex BNCPPt has been constructed. The target model platinum (II) complex BNCPPt shows green emission with a single peak at 497 nm and the quite narrow full-width at half-maximum (FWHM) of 27 nm in toluene.